Carbon Nanotubes for Cold Electron Sources**

By *Pierangelo Gröning,* Pascal Ruffieux, Louis Schlapbach,* and *Oliver Gröning*

Technological advances in the field of microelectronic fabrication techniques have triggered a great interest in vacuum microelectronics. In contrast to solid-state microelectronics, which entails scattering-dominated electron transport in semiconducting solids, vacuum microelectronics relies on the scattering-free, ballistic motion of electrons in vacuum. Since the first international conference on vacuum microelectronics substantial progress in this field has been made. The first technological devices using micrometer-sized electron emitting structures are currently being commercialized. Field-emission flat-panel displays (FED) seem to be an especially promising competitor to LCD displays. Today there is only one mature technology for producing micro-gated field-emission arrays: the Spindt metal-tip process. The drawbacks of this technology are expensive production, critical lifetime in vacuum, and high operating voltage. Carbon nanotubes (CNT) can be regarded as the potential second-generation technology to the Spindt metal micro-tip. In this review we show that the field emission (FE) behavior of CNT can be accurately described by Fowler–Nordheim tunneling and that the field-enhancement factor β is the most prominent factor. Therefore the FE properties of a CNT thin film can be understood in terms of local field enhancement $\beta(x,y)$, which can be determined with scanning anode field emission microscopy (SAFEM). To characterize the FE properties of an ensemble of electron emitters we used a statistical approach (as for thin film emitters), where $f(\beta)d\beta$ gives the number of emitters on a unit area with field-enhancement factors within the interval $[\beta,\beta + d\beta]$. We show that the field-enhancement distribution function $f(\beta)$ gives an almost complete characterization of the FE properties.

1. Introduction

Several electronic devices are based on electron sources. Some familiar examples are cathode ray tubes in television sets, X-ray generators, and microwave amplifiers. In general the electron sources in these devices are thermionic emitters operating at temperatures between 950 and 2000 °C. Although relatively inexpensive and delivering high current densities, thermionic emitters have a number of significant drawbacks. They are power-controlled electron sources (via the temperature) and therefore direct modulation of the electron emission is rather slow. Also, energy consumption is high due to the high operating temperatures, and (most important) miniaturization to micrometer-sized emitters is not possible because of insufficient heat dissipation.

The phenomenon of field electron emission (FE) was first reported by Wood in 1897 and occurs when very high electric fields are present at a surface.[1,2] Under this condition the potential step at the surface confining the electrons to the solid, becomes a potential barrier, which is to a first approximation triangular in shape. The height of the potential barrier is

[*] *Dr. P. Gröning, Dr. P. Ruffieux, Prof. L. Schlapbach, Dr. O. Gröning*
Swiss Federal Laboratories for Materials Testing and Research
Überlandstrasse 129, CH-8600 Dübendorf (Switzerland)
E-mail: Pierangelo.Groening@empa.ch

[**] *This work was financially supported from the Top Nano 21 program of the Commission of Technology and Innovation (CTI), MaNEP a National Centre of Competence in Research from the National Science Foundation, and CANVAD a project of the 5th EU Framework Program.*

 DOI: 10.1002/adem.200310098

given by the work function ϕ and is typically about 5 eV for ordinary metals. When the width of this barrier gets smaller than 2 nm the electrons close to the Fermi energy ε_F have a finite probability of tunneling through the barrier and escaping, as shown in Figure 1.

In 1928 Fowler and Nordheim[3] delivered the first generally accepted explanation of FE in terms of the newly developed theory of quantum mechanics. According to the Fowler–Nordheim theory the FE current density j is a function of the electric field E and the emitter work function ϕ according to the following equation

$$j = \frac{e^3}{4(2\pi)^2\hbar\phi} E^2 \exp\left(-\frac{4\sqrt{2m_e}}{3\hbar eE}\phi^{1.5}\right) \quad (1)$$

The large electric fields of about 3000 Vμm^{-1} required for FE are difficult to generate at flat surfaces, but can be generated by the field-enhancing properties of tip-like structures. The field enhancement at the apex of a needle of height h and radius r is, to a first approximation, equal to the aspect ratio h/r.[4] A carbon nanotube (CNT) with a diameter of 10 nm and a length of 2 μm exhibits therefore a field-enhancement factor β up to 400. So the required electric field of 3000 Vμm^{-1} for FE can be generated at the nanotube apex by a very low applied electric field of 7.5 Vμm^{-1}.

The development of FE electron sources has been hampered for half a century by the fact that field-enhancing tip-like structures are needed to create locally the high electric fields for FE to take place. Usually the higher the field-enhancement factor β, the smaller the effective emission area of the tip becomes, as the radius of curvature decreases. Although the FE current density can easily exceed 10 000 Acm^{-2}, the total emission current per single tip remains small because the emitting area, being the apex of the tip, is small. The current per single tip rarely exceeds 0.1 mA. As a result field emitters are only used where high brightness rather than high currents are required, as in the case of a high-resolution scanning electron microscope (SEM).

The key for reaching field emitters of high current density approaching 1 Acm^{-2} resides in the integration of a large number of field emitters. Depending on the required emission current density, the density of the emitting tips has to be up to 10^8 cm^{-2}. This limits their size to micrometer or even submicrometer dimensions. Today there is only one mature technology for producing micro-gated field-emission arrays: the Spindt metal-tip process (Fig. 2). The drawbacks of this technology are expensive production, critical lifetime in vacuum, and high operating voltage. CNT can be regarded as the potential second-generation technology to the Spindt metal micro-tip. The use of CNT as field-enhancing structures in cold electron sources can bring advantages such as longer lifetime and operation in poor vacuum due to the high chemical inertness as well as low operation voltages and, perhaps most important, very low-cost production techniques.

The ideal cold electron source in a micrometer device has to meet several important requirements.[6]

- The electron source must be capable of being fabricated to submicrometer tolerances so that the emitting area is precisely defined and is geometrically and chemically stable during its operation lifetime.
- The emission current should be voltage controllable, preferably with a drive voltage in the range obtained from „off the shelf" integrated circuits (< 100 V).
- The source must be capable of emitting very high current densities so that the total current emitted from the small available area is sufficient for device operation. Since a current of even 1 μA from 1 μm^2 area requires a current density of 100 Acm^{-2}, a current density of 10 Acm^{-2} is a lower limit for a source to reach wide applications in vacuum microelectronic devices.
- The energy spread of the emitted electrons should be comparable to conventional thermionic cathodes (i.e., < 0.5 eV), or within tolerable limits for the device.
- The emission characteristic should be reproducible from one source to another and should be stable over very long periods of time (10 000 h) for acceptable device lifetimes.

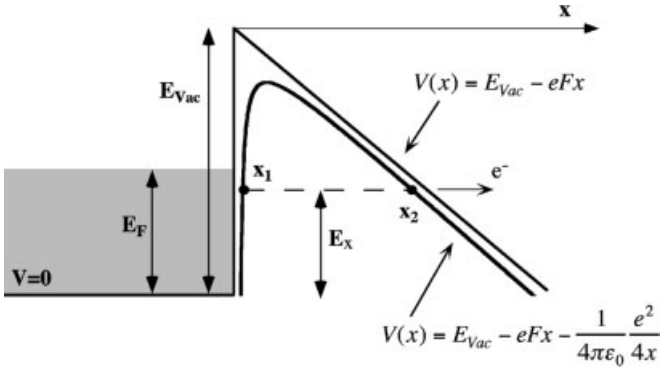

Fig. 1. Schematic illustration of the surface potential barrier under the action of an external electric field.

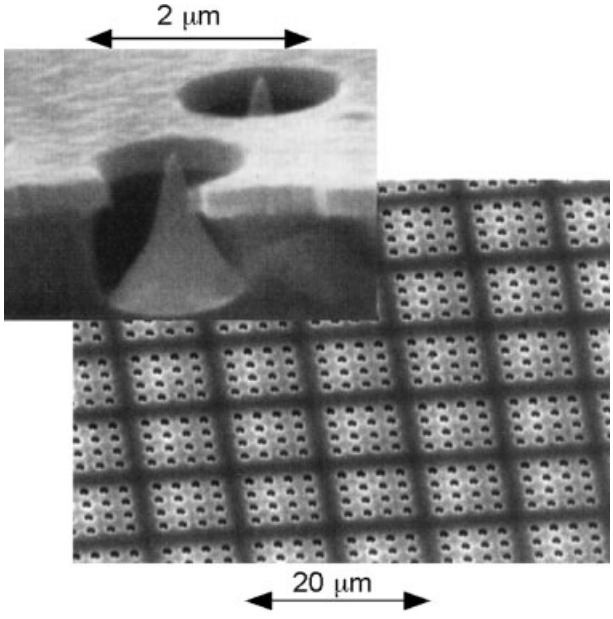

Fig. 2. Field emitter array of evaporated metal tips: Spindt tips [5].

- The cathode must be resistant to unwanted occurrences in the vacuum environment: ion bombardment, reactions with residual gas, temperature extremes, and arcing.
- Cathode manufacturing should be inexpensive, without critical processes, and adaptable for various applications.

Cold electron sources designed as a large number of parallel-operating micrometer-sized electron sources open the door to a large number of interesting technological applications, such as high-power radio frequency amplifiers, flat panel displays, electron guns for klystroms or travelling wave tubes, parallel e-beam lithography, or data storage devices.[7]

2. Experimental

CNT thin films were grown by chemical vapor deposition (CVD) of a C_2H_2/N_2 gas mixture at substrate temperatures around 750 °C on low-resistance p-type Si wafers or by plasma-enhanced CVD (PECVD) of a CH_4/N_2 gas mixture at temperatures of 800–1000 °C. The growth catalyst was either deposited on the substrate by as a thin Ni film (5–10 nm) by sputtering or using a solution of 40 mM $Fe(NO_3)_3$ in ethanol, which was sprayed onto the silicon substrate. Using the CVD process we produced dense CNT films with a mean tube diameter of 30 nm and a preferential orientation normal to the substrate surface.[8,9] The orientation of the individual nanotubes in the film is forced by the tube density. Above a critical density the direction of the growing nanotube is confined by the surrounding growing tubes. Using the PECVD process well-aligned CNT films with controlled length and site density can be produced.[10,11] The mean tube diameter in these films is about 80 nm. Figure 3 shows SEM images of CNT films grown by CVD and PECVD.

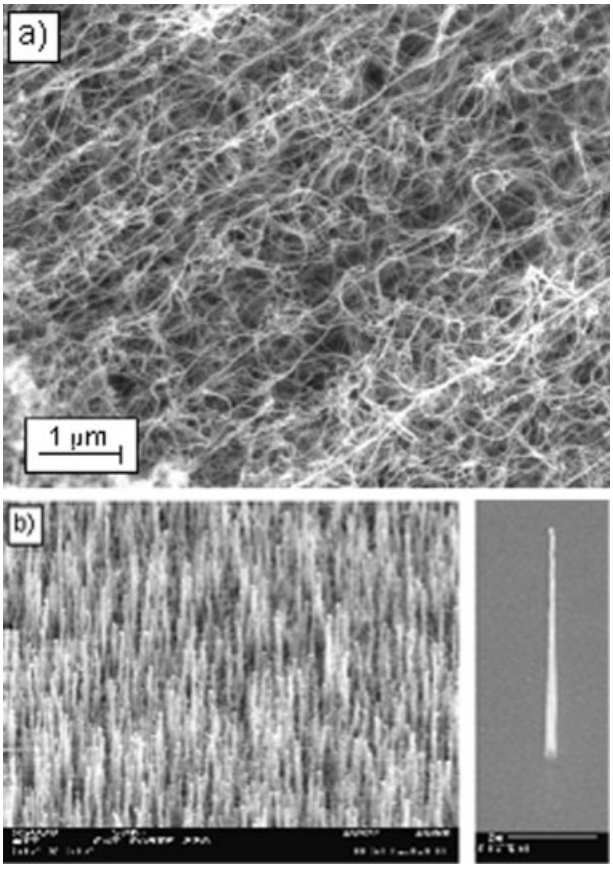

Fig. 3. Carbon nanotube thin films grown by: a) chemical vapor deposition (CVD); b) plasma enhanced chemical vapor deposition (PECVD).

The advantage of the PECVD process compared with the CVD process is that the alignment of the nanotubes is not due to steric repulsion. This allows the growth of well-aligned CNT arrays with controlled site densities, as shown in Figure 4.[12]

Energy-resolved FE measurements were carried out in an OMICRON surface analysis system (base pressure $< 10^{-10}$ mbar) equipped with high energy resolution electron analyzer EA 125 HR.[13] The measurements were carried out in the constant analyzer energy (CAE) mode with a pass energy of 5 eV. With the pass energy of 5 eV and the entrance and exit slits set to minimum, the energy resolution of the analyzer is 35 meV at 100–1000 eV kinetic energy. The high voltage was set to the sample by a Keithley 237 instrument. The ripple on the voltage was always below 5 mV. For field emission spectroscopy (FES) measurements the sample could be tilted and rotated to any polar and azimuthal angle with respect to the electron analyzer axis. This allowed us to set the sample-detector orientation for maximum count rates. The FE spectra were measured between 1 pA and 1 nA total emission current, with count rates of 100 to 10^6 cps.

Whereas a single field electron emitter can be said to be completely characterized in terms of its work function ϕ at the emission site, the field-enhancement factor β, and the resistance R, the description of the overall emission behavior from a thin film emitter with a large number of emission sites requires a statistical approach.[14] The number of degrees of freedom with regard to geometrical alignment, orientation, length, diameter, and inter-emitter distances within the thin film emitter ensemble is much larger than for a single emitter. It can also be expected that ϕ and R exhibit some variation. Electrostatic screening has to be taken into account for thin film emitters, sine the presence of a large number of emitters may affect the local electric field E at the emission sites. The

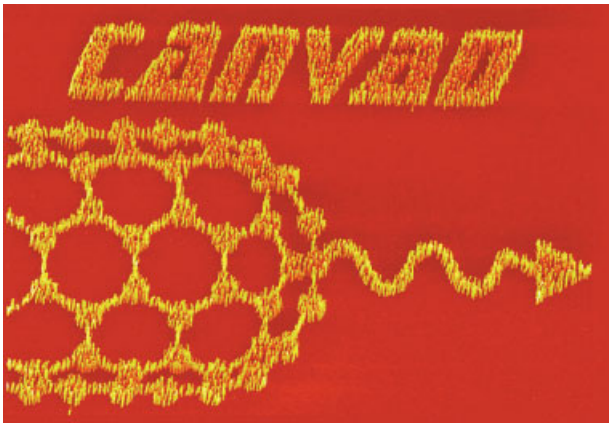

Fig. 4. SEM image (40 µm × 25 µm) of deterministically grown carbon nanotubes (nanofibers) using PECVD showing the name CANVAD a project of the 5th EU Framework Program. (In collaboration with K.Teo and W. Mine from the University of Cambridge).

emission properties can therefore vary considerably from one position to another within the thin film emitter. Therefore the FE behavior of CNT thin films was investigated by means of a home-made vacuum scanning anode FE microscope (SAFEM), operating at a typical base pressure of 10^{-7} mbar.[15] In this set-up the sample is mounted on a computer-controlled piezo-driven x/y translation stage and a tip of radius 1 μm is approached to the sample in steps of 100 nm, and thereafter held at a constant height d. The tip–sample distance d is chosen larger than the surface roughness of the sample under investigation, typically 5–10 μm. The tip–sample distance can be changed without hysteresis. The *FE* current $I(x,y)$ at constant applied voltage or the extraction voltage $V(x,y)$ at constant emission current is mapped as a function of the lateral tip position with the Keithley 237 source–measure unit. We call these two measurement modes the constant voltage mode (CVM) and the constant current mode (CCM). The $I(x,y)$ map obtained in the CVM is analogous to the electron emission on a phosphorous screen, albeit with higher resolution. Sample areas from several square micrometers up to 800 μm × 800 μm can be scanned with submicrometer resolution depending on the tip–sample distance.

The advantage of the SAFEM is that we are not only able to determine the emission site density (ESD) with higher resolution and at higher electric fields, but moreover the dynamic range of the detected emission current is larger than a phosphorous screen. Keep in mind the *I–E* characteristic of FE described by the Fowler–Nordheim relation, Equation 1, small variations in the local electric field or the local field enhancement, are likely to destroy emission sites with high field-enhancement factors β due to elevated current levels. Consequently, emitter degradation can occur during scanning in CVM. To avoid emitter degradation, SAFEM investigations where performed in the CCM. In CCM the emission current is kept constant and the extraction voltage V is measured as a function of tip position. In this case we obtain a $V(x,y)$ map without current saturation effects or emitter degradation. This is experimentally and conceptually neat since the $V(x,y)$ map is actually an inverted image of the field-enhancement landscape $\beta(x,y)$, as shown below.

3. Results and Discussion

Figure 5 shows the electron emission of a CVD-grown CNT film monitored on a phosphorous screen. For an applied field of 2.5 V/μm the emission site density is approximately 10^3 cm^{-2} and increases to its maximum at roughly 3 V/μm when the whole screen is illuminated, making it impossible to determine an emission site density. These electric fields E are extremely low compared with those required for Spindt-type metallic tips, of the order of 100 V/μm. With this integral FE measurement, using a simple diode configuration, it is possible to determine the threshold field E_{th} for electron emission, the current–voltage (*I–V*) characteristic, and with some restrictions also the emission site density. These values are of technological importance but are far from a physically relevant and complete characterization of the electron emission properties of a thin film. The complete and physically relevant characterization of the electron emission properties of a thin film emitter includes the following.

- The determination of the work function ϕ at the emission sites.
- The distribution $f(\beta)$ of the field-enhancement factors β.

3.1. Field Emission Spectroscopy (FES)

As suggested above, current–voltage (*I–V*) measurements are usually used to characterize the electron emission behavior according to the Fowler–Nordheim relation. From these measurements it is not possible to determine the work function ϕ as the relevant parameter for FE. The reason for this is that experimentally one does not measure current–field (*I–E*) characteristics but *I–V* characteristics, where one relates the applied voltage to some applied field, for example, by dividing the applied voltage by the anode–cathode distance. The problem is that this applied field may not correspond to the local field present at the emission site due to field-enhancement effects. Assuming that E_0 ($E = E_0 \cdot \beta$) denotes the applied electric field in FE experiments, the Fowler–Nordheim relation will change to

$$j = \frac{e^3}{4(2\pi)^2 \hbar\phi} E_0^2 \beta^2 \exp\left(-\frac{4\sqrt{2m_e}\phi^{1.5}}{3\hbar \cdot eE_0\beta}\right) \quad (2)$$

The total energy distribution $P(\varepsilon)$ of the field emitted electrons near the Fermi energy ε_F can be written as

$$P(\varepsilon) = f(\varepsilon, \varepsilon_F, T) B(E, \phi) \exp\left[C_v \frac{\phi^{0.5}}{E}(\varepsilon - \varepsilon_F)\right] \quad (3)$$

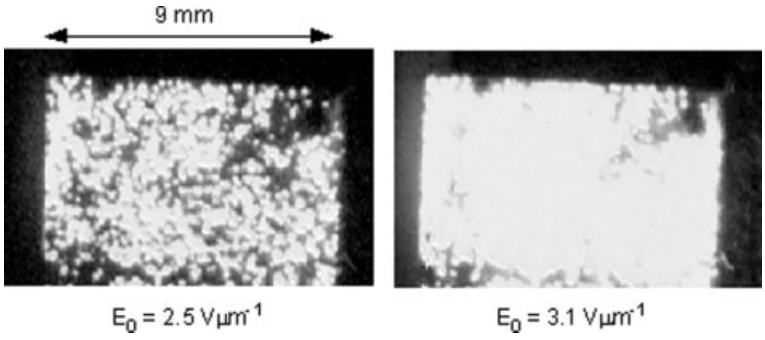

Fig. 5. Electron FE pattern from a CVD-grown CNT film monitored by a phosphorous screen. The images are taken at 2.5 and 3.1 V/μm applied electric fields. The size of the image is 1.1 cm× 0.7 cm.

with $C_v = \frac{2\sqrt{2m_e}}{e\hbar}$

where ε denotes the electron energy and $f(\varepsilon,\varepsilon_F,T)$ stands for the Fermi–Dirac distribution at temperature T and $B(E,\phi)$ is an energy-independent intensity factor. FES is ideally suited to checking the validity of the Fowler–Nordheim theory for CNT emitters. Figure 6 shows a series of FE spectra measured from a sample of multiwall carbon nanotubes (MWCNT) recorded at room temperature at different applied voltages and therefore different applied fields, E_0. For all spectra the applied voltage was subtracted from the kinetic energy scale giving the energy of the emitted electrons relative to the Fermi energy ε_F. The solid lines are the best fit to the data using Equation 3. By integrating the spectra over the energy we obtain a value that is proportional to the emission current. According to the Fowler–Nordheim theory the plot of $\ln(j/E^2)$ against $1/E$ or more generally $\ln(I/V^2)$ against $1/V$ should yield a straight line with negative slope. As can be observed from the inset in Figure 6, the I–V characteristic of the MWCNT emitter obeys the Fowler–Nordheim law. These results of the FES investigation on MWCNT therefore show that the Fowler–Nordheim theory describes perfectly the emission behavior at room temperature with regard to the I–V (or I–E) characteristic as well as with regard to the energy distribution of the field emitted electrons. A more detailed analysis of the FE spectra allows the determination of the emitter work function, ϕ, which (together with the emitting area) is the main parameter describing the I–V characteristic. In the case of MWCNT we can consistently determine a work function ϕ = 4.9 ± 0.3 eV.[9,16] To summarize the results from FES investigations one can state that the FE behavior at room temperature of MWCNT is analogous to a metallic tip with a 4.9 eV work function. Therefore also in the case of MWCNT emitters the local electric fields present at the nanotube apexes must be of the order of 4000 Vμm^{-1} in order to achieve technologically relevant emission currents of 100 nA per single emitter.

3.2. Environmental Stability

The term environmental stability is used to describe the interaction of electron emitters with the gaseous environment in which they are operated. Such interactions typically lead to emission current fluctuations on a time scale of seconds to minutes. If the current fluctuations are large they may negatively affect device performance. In addition, the long-term stability is dependent on emitter interactions with the environment, so investigations on environmental stability are important. Such investigations have been done in the past on etched metal tips using FE microscopy. The FE microscope (FEM) invented by Müller[17] in 1937 has for a long time been the state of the art for investigating adsorption and diffusion phenomena at surfaces, with almost atomic resolution.

Figure 7 shows FEM patterns commonly observed from SWCNT and MWCNT. These emission patterns are not stable in time but switch from one configuration to an other. The switching frequency increases with increasing currents and is of the order of 1 Hz. Associated with this instability of the emission spot are fluctuations in the emission current, as indicated by the different intensities of the emission patterns in Figure 7b. Each emission pattern has a well-defined emission current for a given applied voltage. Therefore, the emission current fluctuates between different current levels associated with different emission patterns. The difference between the

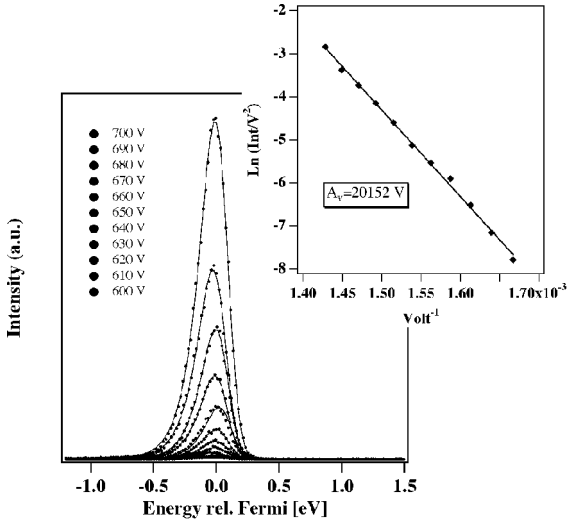

Fig. 6. Series of field emitted total energy distribution from a single MWCNT at different applied voltages and therefore at different applied electric fields. The spectrum measured at 700 V exhibits the largest intensity. The solid lines are the best fits to the experimental data using Equation 3. The inset displays the Fowler–Nordheim plot of the integrated spectral intensity yielding a straight line as expected from theory.

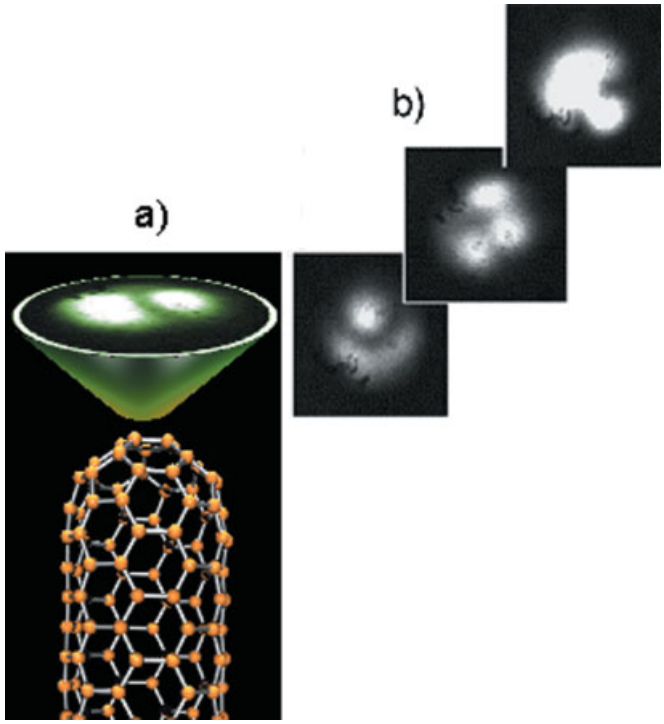

Fig. 7. a) Schematic illustration of CNT with the lobed FEM pattern of a MWCNT at 300 K. b) Some examples of a large variety of FEM pattern commonly observed from singlewall CNT (SWCNT) and MWCNT [13].

highest and lowest current level can be up to a factor of ten. Such random telegraphic noise was observed by different groups.[16,18] It is recognized that the FEM patterns on the screen reflect the electronic structure, the anisotropy of the work function, local variation of the microscopic field, and electron transmission probability of a CNT cap. This means that atomically sized areas on the CNT cap, where the work function is lower or the local electric field is higher than the surrounding regions, are reproduced with higher intensity on the phosphor screen. Therefore the different emission patterns of CNT can be understood in terms of switching between different states with relatively small energy difference in levels close to the Fermi energy. It seems plausible to think that energy levels of the CNT at the apex are modified through adsorbed molecules coming from the gas phase during FE. Sometimes adsorption is very firm and may result in a resonant tunneling state, which can lead to increased tunneling probability and anisotropy in the FE current.[19] We observed that the FE fluctuations are not sensitive to H_2 and H_2O, the two main components of residual gases in vacuum systems, up to 10^{-4} mbar gas pressure. Increased partial pressure of O_2 causes degradation of FE due to reactive ion etching. The suggestion of Rinzler et al.[18] that the emission fluctuations are due to individual desorption processes induced by ion bombardment seems very convincing.

Defects and adsorbates are known to play an important role in the modification of electronic states of solids, particularly for 2D systems. As a model for CNT we used graphite to study changes in the electronic structure due to point defects and adsorbates. We used combined mode scanning tunneling microscopy (STM) and atomic force microscopy (AFM) to study both topographic and electronic changes on graphite in the vicinity of defects created by atomic hydrogen.[20] In summary, our studies of the interaction of hydrogen ions with the graphite surface by means of AFM/STM and photoelectron spectroscopy reveal chemisorption of hydrogen and atomic vacancy formation. Both modifications result in local charge enhancement and long-range perturbations of the electronic structure consisting of a $(\sqrt{3} \times \sqrt{3})R\,30^\circ$ superstructure in the local density of states (LDOS). The range of the modified electronic structure induced by one chemisorbed H atom or by one atomic vacancy is of the order of 6 nm or 20–25 lattice constants (Fig. 8). These results show the fundamental importance of adsorbates and point defects on CNT for their FE properties.

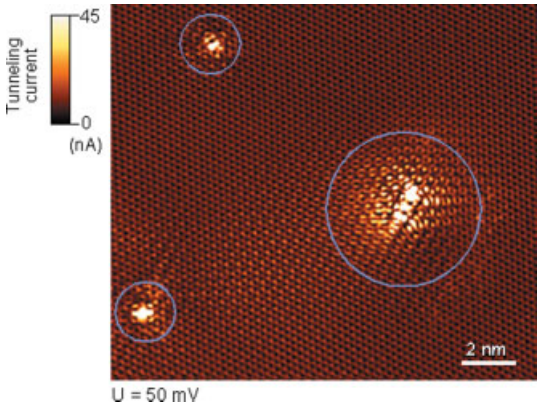

Fig. 8. Recorded current image of an AFM measurement showing single point defects on the graphite surface created by H_2 plasma treatment. Measurement parameters: force setpoint, 2 nN; sample bias, 50 mV.

3.3. Characterization of Carbon Nanotube Thin Film Emitters

Whereas a single field electron emitter can be said to be completely characterized by its work function ϕ at the emission site, the field-enhancement factor β, and the resistance R, the description of the overall emission behavior from a thin film emitter with a large number of emission sites requires a statistical approach.[14] The number of degrees of freedom of geometrical alignment, orientation, length, diameter, and inter-emitter distances within the thin film emitter ensemble is much larger than for a single emitter. It can also be expected that ϕ and R exhibit some variation. Electrostatic screening has to be taken into account for a thin film emitter, sine the presence of a large number of emitters may affect the local electric field E at the emission sites. The emission properties can therefore vary considerably from one position to another within the thin film emitter.

Thin film electron emitters are often characterized by a „threshold" field E_{th} required to obtain a given FE current density in a typical large anode diode type FE experiment. Such characterization can be misleading since a cathode with a spatial extension in the square millimeter range may contain a small number (sometimes only one) of strong emitters and thus can have a low threshold field E_{th}, which obviously will not guarantee a high emission current density, because the emitter ensemble shows a certain distribution of the field-enhancement factor β and, therefore, the emission current density. In this picture the FE properties of a thin film must be represented by a function $f(\beta)$, where the number of emitters dN on a surface area A with field-enhancement factors in the interval $[\beta,\beta + d\beta]$ is given by

$$dN(\beta) = A \cdot f(\beta) \cdot d\beta \tag{4}$$

Where $f(\beta)$ is the field-enhancement distribution function defined as

$$f(\beta) = \frac{1}{A}\frac{dN}{d\beta}\ [\text{emitter/cm}^2] \tag{5}$$

According to the definition, $f(\beta)$, is proportional to the probability of the field-enhancing structures in the interval $[\beta,\beta + d\beta]$ per unit area. Consequently one may view $f(\beta)$ as a probability distribution. Assuming the same relation for the emission current as a function of the local field F at the emission site for all emitters of the thin film, the FE properties are completely determined by the FE distribution function $f(\beta)$.

In terms of the Fowler–Nordheim relation the assumption of a general relation for the current–field dependence of the electron emission means that all emitters have the same emit-

ting area and the same work function ϕ. The assumption that the work function ϕ is constant for all emitters can partially be justified by the fact that the emitters consist of the same material. Actually, we have found by FES that the work function at the emission site of carbon based materials is always in the range 4.7–5.1 eV. The argument that the emission area should be constant can for CNT be partially justified by the fact that all the emitters are of the same dimensions.

With the field-enhancement distribution function $f(\beta)$ it is now possible to determine immediately the threshold field E_{th} and the emission site density (EDS). The threshold field E_{th} can be determined from

$$I_{th} = A\int_0^\infty f(\beta)\cdot I(\beta,E_{th})d\beta = A\cdot\frac{1.5\cdot10^{-6}}{\phi}\exp\left(\frac{10.4}{\phi^{0.5}}\right)\cdot\int_0^\infty d\beta\cdot f(\beta)\cdot E_{th}^2\cdot\beta^2\cdot\exp\left(-6.44\cdot10^7\frac{\phi^{1.5}}{E_{th}\cdot\beta}\right) \quad (6)$$

Here A denotes the surface of the cathode under investigation. It is worth noting that the threshold field E_{th} will depend on the cathode area, which is measured, so that it is only sensible to define the threshold field E_{th} with regard to a given emission current density j_{th}. In other words, the measured threshold field E_{th} decreases with increasing surface area measured. The characterization of the emission properties of a thin film emitter just by stating the threshold field E_{th} is therefore very questionable.

The emission site density (ESD), which gives the number of active emitters per unit area at a given applied field or voltage is one of the key parameters in characterizing the FE performance or quality of a planar FE cathode. An active emitter is an emitter giving an emission current larger than some threshold current, such as 10 nA. Therefore the ESD as function of the applied electric field E_0 can be calculated from the field-enhancement distribution function $f(\beta)$ by

$$ESD(E_0) = \int_{\beta_{\min}=E_{\min}/E_0}^{\infty} f(\beta)d\beta \ [\mathrm{cm}^{-2}] \quad (7)$$

E_{min} is the local field at the emission site required to produce a minimum detectable emission current I_{min}. In an experimental set-up using a phosphorous screen I_{min} corresponds to the minimum emission site current, required to observe the emission spot by eye.

The emission current density is calculated in a similar manner

$$j(E_0) = \int_0^\infty f(\beta)\cdot j(\beta,E_0)d\beta \ [\mathrm{Acm}^{-2}] \quad (8)$$

As shown, knowledge of the field-enhancement distribution function $f(\beta)$ gives an almost complete characterization of FE behavior of thin film emitters. Therefore, the experimental characterization of thin film emitters should include the determination of $f(\beta)$. The field-enhancement distribution function $f(\beta)$ can be obtained from the spatial distribution of field-enhancement factors β the so-called field-enhancement map $\beta(x,y)$. In theory $\beta(x,y)$ can be calculated from the topography of the surface $h(x,y)$, for example, by solving the Poisson equation at the surface. However, in general the Poisson equation can not be solved because it is extremely difficult to measure $h(x,y)$ with nanometer resolution. Therefore another method is used to derive $\beta(x,y)$. Through Equation 2 the emission current I is directly related to field-enhancement factor β, therefore the local emission current $I(x,y)$ for a thin film emitter is given by

$$I(x,y) = A\cdot\frac{1{,}5\cdot10^{-6}}{\phi}\cdot E_0^2\cdot(\beta(x,y))^2\exp\left(\frac{10.4}{\phi^{0.5}}\right)\exp\left(-6.44\cdot10^7\frac{\phi^{1.5}}{E_0\cdot\beta(x,y)}\right) \quad (9)$$

Hence, the measurement of $I(x,y)$ could theoretically be used to calculate $\beta(x,y)$.

As already discussed, in order to derive $\beta(x,y)$ and avoid current saturation effects, not to say emitter destruction, the scanned electron emission measurement has to be performed in the constant current mode (CCM). In the CCM the voltage applied to the anode is varied as a function of the anode position over the thin film emitter, in order to maintain the same emission current for every point. If the current is reasonably low (about 50 nA), one will obtain a spatially resolved FE image of the extraction voltage $V(x,y)$, without current saturation effects or emitter destruction. This is both experimentally and conceptually beautiful since $V(x,y)$ is actually an inverted image of the field-enhancement landscape $\beta(x,y)$, according to

$$\beta(x,y) = \frac{d\cdot E}{V(x,y)} \quad (10)$$

where d is the tip sample distance and E the local field at the emission site required for a fixed emission current I predicted by the Fowler–Nordheim relation, Equation 2.

Figure 9 displays a high-resolution field-enhancement $\beta(x,y)$ map derived from a SAFEM voltage $V(x,y)$ map recorded at a tip–sample distance of 2–3 μm and 11 nA emission current, on a CVD-grown randomly oriented CNT thin film. The blue diamonds indicate the position of the emission sites with a field-enhancement factor larger than 130. In the map 164 such emitters could be detected on a sample area of 2.4×10^{-5} cm^2 resulting in an ESD of 6.8×10^6 cm^{-2}. The field enhancement was determined using the assumption that the local electric field E present at the nanotube apex is 3800 V μm^{-1} in order to emit 11 nA, as predicted by the Fowler–Nordheim theory. A field enhancement larger than 130 therefore means that the applied electric field E_0 is less than 30 V μm^{-1}. So that we can conclude that for randomly orient-

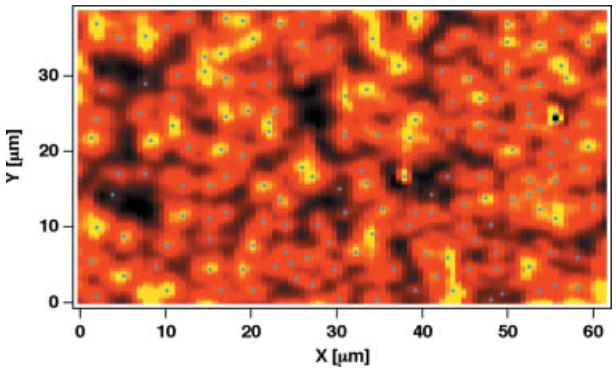

Fig. 9. High-resolution scanning anode field-enhancement map $\beta(x,y)$ on a CVD-grown MWCNT cathode. at a tip-sample distance of 2–3 mm and at a constant emission current of 11 nA. The blue diamonds indicate the position of emission sites. In the map yellow indicates high and black low field enhancement.

ed MWCNT thin films an ESD of 5×10^6 cm^{-2} can be achieved at applied electric fields of the order of 30 V µm^{-1}. This investigation demonstrates that relatively crude, as-deposited CNT thin films already have the potential to achieve technologically relevant emission site densities at moderate applied electric fields. However, it is important to point out that the high emission site density indicated above of a few million per square centimeter is to a certain extent academic as it cannot be exploited on larger cathode area when the electric field is applied in parallel to the CNT emitters.

The reason for this is the large spread of the field-enhancement factor β that the individual emitters exhibit for non-oriented CNT thin films. This has to be related to the fact that a difference of a factor of two in the field enhancement leads to a difference of 103–104 in the emission current at the same applied electric field. We have shown that the emitters on randomly oriented CNT cathodes have an exponential frequency distribution of the following type

$$f(\beta) = C_1 \exp(-C_2\beta) \tag{11}$$

where C_1 and C_2 are positive constants and $f(\beta)\mathrm{d}\beta$ gives the number of emitters per unit area having a field-enhancement factor b in the interval $[\beta,\beta + \mathrm{d}\beta]$. This kind of field-enhancement distribution results in the situation that on a large cathode area (e.g., 1 cm^2) there are a few very strong emitters of very high field enhancement, typically about 1500, which result in the low threshold field E_{th} = 1–2 Vµm^{-1}. However, the ESD at the threshold field is very low, only 1–10 cm^{-2}. Upon an increase in the applied electric field the ESD increases rapidly, but at the same time the emission current from the first few emitters increases exponentially. With further increase of the applied electric field the point is reached where the emission current of the first few strong emitters is so large that they are destroyed. From this point on, the ESD hardly increases as a situation is reached where the appearance of new emitters is balanced by the disappearance of old emitters with increasing applied electric field. For as-deposited MWCNT thin films this point is reached typically at about 10 Vµm^{-1} with an ESD of about 10 000 cm^{-2} and an emission current density of 1–10 mAcm^{-2}. It is clear that under such circumstances the cathode suffers irreversible degradation and that the operation of a cathode under such conditions is highly critical from the point of view of stability and lifetime.

It is crucial to note that emitter degradation at low applied electric fields is the limiting factor for the FE performance of CNT cathodes. To enhance the FE performance of such cathodes a detailed understanding of the degradation mechanism and subsequently the improvement of the degradation behavior is required.

Figure 10 shows the SAFEM field-enhancement map $\beta(x,y)$ of a randomly oriented MWNT thin-film emitter, with regions that have suffered high emission current degradation previously. The region from x = 0 µm to x = 55 µm has been strained with 1.5 µA and the region from x = 55 µm to x = 110 µm has been strained with 2 µA emission current by the SAFEM. The region x > 110 µm has not been current strained. After current straining a field-enhancement map $\beta(x,y)$ was

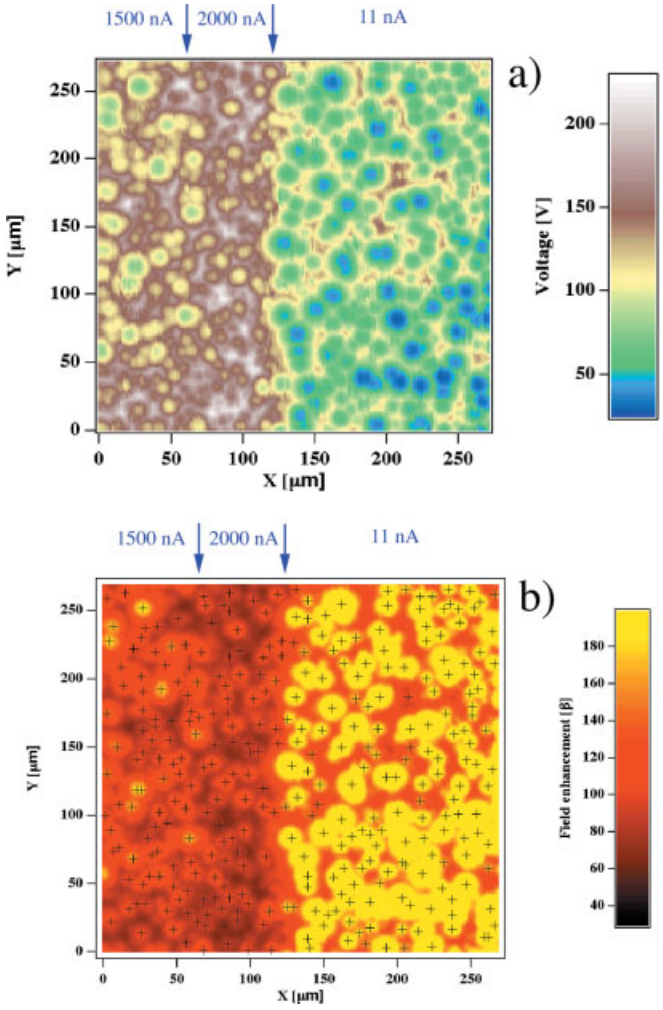

Fig. 10. SAFEM extraction voltage map $V(x,y)$ and corresponding field-enhancement map $\beta(x,y)$. of a randomly oriented MWCNT thin film with two high emission current strained regions on the left hand side. The measurements were performed at a tip-sample distance of 4–5 µm and a constant emission current of 11 nA. Prior to the measurement the regions indicated by the arrows were strained by high emission currents of 1.5 and 2 µA.

recorded at 11 nA and a tip–sample distance of 4–5 μm. One can observe that in the current-strained regions the emitters with a high field-enhancement factor β have been removed, whereas they are still present in the unstrained region. The values at which the current degradation occurs can vary from 500 nA up to a few μA, which is more than 100 times lower than for a single CNT welded on a metal tip. *I–V* measurements on two point contacted CNTs have shown that straight and probably defect-free CNTs, can conduct currents up to 3 mA ballistically without heat dissipation.[21,22]

The emitters that are then left over with a lower field-enhancement factor β are typically very stable and robust, which means that they can sustain emission currents well above 1 μA even up to 100 μA for short periods of time. A closer inspection of the regions strained by 1.5 and 2 μA shows that the average field enhancement is higher in the region strained with the lower current. This behavior indicates that high current degradation is linked with enhancement, where the critical current for degradation decreases with increasing field enhancement and therefore increasing aspect ratio.

Figure 11 shows the *I–V* characteristic of a single emitter on MWCNT thin film cathode. The *I–V* characteristic shows that an irreversible degradation occurs abruptly at 2.2 μA at an applied voltage of 290 V (corresponding to an applied electric field of 14.5 $V\mu m^{-1}$). The degradation manifests itself by a current drop of almost three orders of magnitude, which corresponds to a decrease in the field-enhancement factor β from 630 to 350. It has to be pointed out that most probably the emission after the degradation does not originate from the same tube as before but from a tube nearby, which was before concealed by the original emitter.

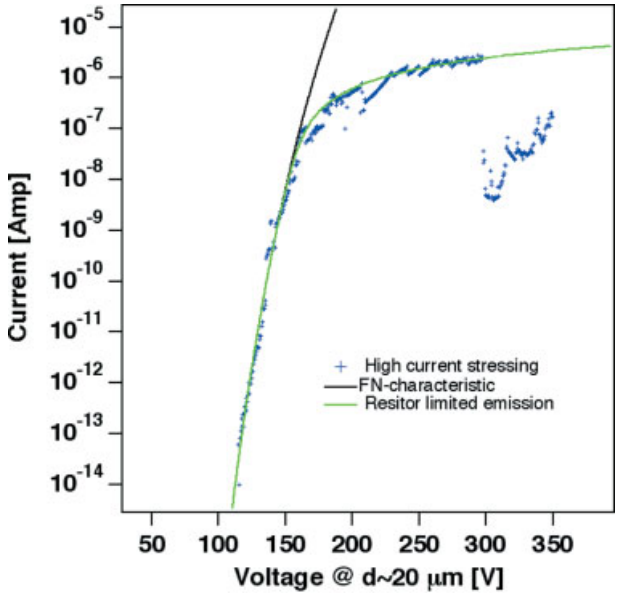

Fig. 11. I–V characteristic of a single emitter on a CNT cathode showing the event of a high current degradation. The blue crosses indicate the experimental data, the black solid line the theoretical Fowler–Nordheim behavior and the green solid line the resistor-limited I–V characteristic.

The black curve in Figure 11 indicates the theoretical Fowler–Nordheim law, Equation 1. One can see that in the low-current regime the measured *I–V* characteristic is well described by the Fowler–Nordheim law. However, above an emission current of about 100 nA a pronounced deviation from the Fowler–Nordheim behavior can be observed. The emission behavior outside the Fowler–Nordheim regime can be modeled using a resistor limitation approach, where it is assumed that there is a voltage drop between the emission site (being the CNT apex) and the electron reservoir (being the electrical contact of the CNT on the substrate). This results in the situation that not the full applied voltage generates the extraction field F for the electron emission, but that this voltage is reduced by the product of the emission current and the resistance in the current path. Assuming an ohmic resistor the high voltage behavior in Figure 9 can be modeled reasonably well by the following relation

$$I = C_1 \cdot (V - \Delta V)^2 \exp\left(-\frac{C_2}{V-\Delta V}\right)$$

$$= C_1 \cdot (V - R \cdot I)^2 \exp\left(-\frac{C_2}{V-R\cdot I}\right) \qquad (12)$$

C_1 and C_2 are positive constants in Equation 12, which is equivalent to the Fowler–Nordheim law, Equation 1 taking into account the proportionality between the voltage and the field. Equation 12 is of course recursive and has to be evaluated numerically. From the emission current and the voltage drop one can estimate the power dissipated in the resistor. In principle the voltage drop could be determined from the model, it has to be stressed, however, that to do so the influence of the voltage drop on the local field at the apex of the tube should be known. This in turn requires information on the exact location of the voltage drop in the current path and the amount of electrostatic shielding the emitter experiences. Both are generally unknown. The possible origins for the resistor-limited emission regime are either a high internal resistance of the CNT, due to defects for example, or a high contact resistance from the substrate to the CNT. It can be estimated that the voltage drop in the resistor-limited regime has to be of the order of 10 V, which gives, with an emission current of 2 μA, a power of 20 μW dissipated. Taking into account the small volume of the contact of 5 $\times 10^{-17}$ cm^{-3}, which is of the order of the CNT diameter to the power of three, one can estimates a power density of about 10^{12} Wcm^{-3} dissipated in the contact. This can easy explain the emission degradation and the observed local substrate melting due to high emission currents. From this consideration it becomes obvious that operating the emitter in the current saturation regime is always risky as the current saturation is a sign of power dissipation and therefore of possible degradation. From the *I–V* curve in Figure 9 it becomes apparent that the voltage window where the emitter can be operated usefully with an emission current between 10 nA and 2 μA is rather small. This finding can be related generally to CNT emitters

by realizing that the window of operation for an emitter corresponds to about twice the threshold filed. Together with the large spread in the field-enhancement distribution function $f(\beta)$, this leads to the limitation in the emission performance of randomly oriented CNT thin film emitters. The threshold field of macroscopic CNT thin film emitters of 1 cm^2 area is generally around 2 $V\mu m^{-1}$, SAFEM investigations, however, show that an interesting emission site density (ESD) of the order of 10^6 cm^{-2} is reached only for applied fields higher than 25 $V\mu m^{-1}$. According to the considerations above, emitter degradation has to be expect for applied fields around 5 $V\mu m^{-1}$. It is therefore not possible to reach the required applied field for the high ESD without very severe emitter degradation!

4. Conclusions

Significant progress in the understanding of electron emission has been achieved since the first reports on low-threshold field electron emission from carbon thin film emitters in the early nineties. It seems certain that the low threshold field electron emission from carbon thin film electron emitters can be accurately described by Fowler–Nordheim tunneling. Fowler–Nordheim tunneling requires high electric fields of the order of 3000 V/μm generated by field-enhancing structures.

Contrary to a single emitter, the emission properties of a thin film emitter requires a statistical treatment, since the field-enhancing structures exhibit a distribution with regard to the filed enhancement β. Therefore the electron emission properties of thin film emitter with an ensemble of field-enhancement structures have be characterized in terms of the spatial field enhancement, the field-enhancement map $\beta(x,y)$. The variation in β for different field-enhancement structures leads to a β distribution, the field-enhancement distribution function $f(\beta)$, which can be seen as a probability function of the field-enhancing structures. The field-enhancement distribution function $f(\beta)$ can be said to give an almost complete characterization of the FE properties, contrary to the threshold field E_{th}, of thin film emitters. In order to obtain a FE device with uniform brightness and high emission site density from thin films, stringent requirements must be placed on the permitted spatial variation of the emitting sites and therefore the variation of the field enhancement β. Homogeneous electron emission from an ensemble of field emitting structures, defined as $dI/I < 50$, requires a relative variation of the field enhancement $d\beta/\beta$ of less than 4 %. Therefore, it is desirable to optimize the density of sites close to the highest field enhancement of the ensemble to the limit of electrostatic screening effect. The example of CNT based field electron emission technology demonstrates clearly the difficult path from *Nanoscience* to *Nanotechnology*.

Received: June 02, 2003

[1] J. W. Gadzuk, *Rev. Mod. Phys.* **1973**, *45*, 487.
[2] R. W. Wood, *Phys. Rev. Ser. I* **1897**, *5*, 1.
[3] L. W. Nordheim, *Proc. Roy. Soc. London, Ser. A* **1928**, *121*, 626.
[4] F. Rohrbach, *CERN Report 71-5/TC-L*, **1971**.
[5] P. R. Schwoebl, I. Brodie, *J. Vac. Sci. Technol. B* **1995**, *13*, 1391.
[6] I. Brodie, C. Spindt, *Adv. Electronics Electron Phys.* **1992**, *83*, 6.
[7] Hewlett Packard, *Sci. Am.* **2000**, *May*, 50.
[8] H. Kind, J.-M. Bonard, Ch. Emmenegger, L.-O. Nilsson, K. Hernadi, E. Maillard Schaller, L. Schlapbach, L. Forro, K. Kern, *Adv. Mater*. **1999**, *11*, 1285.
[9] O. Gröning, O. M. Küttel, C. Emmenegger, P. Gröning, L. Schlapbach *J. Vac. Sci. Technol. B* **2000**, *18*, 665.
[10] M. Tanemura, K. Iwata, K. Takahashi, Y. Fujimoto, F. Okuyama, *J. Appl. Phys.* **2001**, *90*, 1529.
[11] Y. Tu, Z. P. Huang, D. Z. Wang, J. G. Wen, Z. F. Ren, *Appl. Phys. Lett.* **2002**, *80*, 4018.
[12] K. B. K. Teo, M. Chowalla, G. A. J. Amaratunga, W. I. Milne, D. G. Hasko, G. Pirio, P. Legagneux, F. Wyczisk, D. Pribat, *Appl. Phys. Lett.* **2001**, *79*, 79.
[13] P. Riffieux, P. Schwaller, O. Gröning, L. Schlapbach, P. Gröning, Q. C. Herd, D. Funnemann, J. Westermann, *Rev. Sci. Instrum.* **2000**, *71*, 3624.
[14] L. O. Nilsson, PhD Thesis No. 1337, Physics Department, University of Fribourg, Switzerland **2001**.
[15] L. Nilsson, O. Gröning, O. M. Küttel, P. Gröning, L. Schlapbach, *J. Vac. Sci. Technol. B* **2002**, *20*, 326.
[16] O. Gröning, PhD Thesis No. 1258, Physics Department, University of Fribourg, Switzerland **1999**.
[17] E. W. Müller, *Z. Phys.* **1937**, *106*, 541.
[18] A. G. Rinzler, J. H. Hafner, P. Nikolaev, L. Lou, S. G. Kim, D. Tomanek, P. Nordlander, D. T. Colbert, R. E. Smalley, *Science* **1995**, *269*, 1550.
[19] K. Dean, B. R. Chalamala, *Appl. Phys.* **1999**, *85*, 3822.
[20] P. Ruffieux, O. Gröning, P. Schwaller, L. Schlapbach, P. Gröning, *Phys. Rev. Lett.* **2000**, *84*, 4910.
[21] S. Frank, P. Poncharal, Z. L. Wang, W. A. de Heer, *Science* **1998**, *280*, 1744.
[22] A. Zettel, J. Cumings, in *Proc. XIV Int. Winterschool Electronic Properties of Novel Materials*, Kirchberg, Tirol, Austria **2000**, p. 526.

